Available online at www.sciencedirect.com
SCIENCE DIRECT
Journal of Sound and Vibration 295 (2006) 1085–1098
JOURNAL OF SOUND AND VIBRATION
www.elsevier.com/locate/jsvi

Short Communication

A novel sensor for measuring the acoustic pressure in buried plastic water pipes

J.M. Muggleton*, M.J. Brennan, R.J. Pinnington, Y. Gao

Institute of Sound & Vibration Research, Southampton University, Highfield, Southampton, SO17 1BJ, UK

Received 22 February 2005; received in revised form 4 January 2006; accepted 4 January 2006
Available online 17 April 2006

Abstract

Acoustic techniques are widely used to locate leaks in buried water pipes. However, difficulties are often encountered when attempting to detect a leak in a plastic pipe, as the leak noise signals attenuate very rapidly away from the leak. Identifying suitable sensors which can be easily deployed and are sufficiently sensitive has been problematic. Polyvinylidene fluoride (PVDF) wire ring sensors have been proposed and demonstrated successfully in laboratory conditions previously. Here it is proposed that the ring sensor is used in a modified configuration: a flexible hose instrumented with the ring sensor is connected to the pipe, via a fire hydrant or other standard access point. Some theoretical modelling has been carried out, which predicts that the acoustic pressure in the main pipe transmits well into the sidebranch, whilst the pressure in the main pipe is largely unaffected. This suggests that PVDF wire located on the sidebranch will effectively monitor the pressure in the main pipe. Moreover, if the sidebranch is sufficiently flexible, substantial sensitivity gains can be made using this configuration compared with locating the wire on the main pipe. Measurements made in the laboratory on a medium density polyethylene (MDPE) finite pipe with a polythene sidebranch connected to it confirm that the acoustic pressure in the main pipe can indeed be measured on the sidebranch. The expected sensitivity gains were not fully realized, and a number of different reasons for this are proposed.

1. Introduction

Detection of water leaks in buried pipes is currently a topic of concern in the UK and across the world because of decreasing water supplies due to changing rainfall patterns, deterioration of antiquated distribution systems, and an ever-increasing population. Furthermore, leaks are considered to be a public health issue as every puncture in the main is a potential entry point for contaminants.

The use of acoustic methods to find leaks, as described by Fuchs and Riehle [1], is now common practice in many countries. Correlation techniques are generally used, and although these techniques have been successful for many years when used with metal pipes, difficulties are often encountered when attempting to detect a leak in a plastic pipe. These have been examined, to some extent by Hunaidi and Chu [2,3]. The leak noise signals

*Corresponding author. Tel.: +44 23 8059 2936; fax: +44 23 8059 3190.
E-mail address: jm9@soton.ac.uk (J.M. Muggleton).

0022-460X/$ - see front matter © 2006 Elsevier Ltd. All rights reserved.
doi:10.1016/j.jsv.2006.01.032

attenuate very rapidly away from the leak, and so may be extremely small. Identifying suitable sensors which can be easily deployed and are sufficiently sensitive has been problematic.

Polyvinylidene fluoride (PVDF) wire ring sensors, which monitor the circumferential strain in the pipe wall (proportional to the internal acoustic pressure at low frequencies), have been proposed and demonstrated successfully by Pinnington and Briscoe [4] and Muggleton et al. [5,6] in laboratory conditions and, to a limited extent, in the field by Muggleton et al. [5]. The pressure sensitivity of the sensor is proportional to the number of turns around the pipe, so within reasonable limits can be increased as much as is needed. Unfortunately, in many parts of the water distribution system, not all of the circumference of the pipe is accessible, so the sensor cannot be effectively positioned around the pipe.

In this paper, it is proposed to use the ring sensor in a modified configuration. A flexible hose instrumented with the ring sensor is connected to the pipe, via a fire hydrant or other standard access point. Some theoretical modelling is carried out to determine the sensitivity of this type of sensor to pressure fluctuations in the main pipe. This is supported by experimental work to validate the theoretical findings. The anticipated advantage of this type of sensor over a conventional hydrophone is that it would be relatively cheap, simple to deploy on a pipe in situ, and potentially could be an extremely sensitive pressure-measuring device.

A theoretical model of a buried fluid-filled pipe to predict both wavespeed and attenuation has been developed and validated previously by Muggleton et al. [5–8], developing on earlier work on an in-vacuo pipe by Pinnington and Briscoe [4]. Acoustic energy in buried water pipes generated by a leak propagates at relatively low frequencies, generally less than a few hundred Hz [1–3], and so it is the low frequency dynamics of the system, well below the ring frequency of the pipe, that is of interest. In this frequency range, four wave types are responsible for most of the energy transfer [4,9]: three axisymmetric waves, $n = 0$, and the $n = 1$ wave, related to beam bending. Of the $n = 0$ waves, the first, termed $s = 1$, is a predominantly fluid-borne wave; the second wave, $s = 2$, is predominantly a compressional wave in the shell; the third wave, $s = 0$, is a torsional wave uncoupled from the fluid. Correlation measurements indicate that leak noise propagates predominantly as the axisymmetric $s = 1$ wave, so it is this wave which is of most interest in this context.

2. Axisymmetric 'fluid-dominated' wavenumber

The pipe equations for $n = 0$ axisymmetric wave motion for a fluid-filled pipe, both in-vacuo and surrounded by an infinite elastic medium have been derived previously [4,7] and expressions for the wavenumbers for the $s = 1$, fluid-dominated, and $s = 2$, shell-dominated, waves have been found. The derivations are based on simplified forms of Kennard's equations [10] with shell bending neglected, so are only valid below the pipe ring frequency. Furthermore, it is assumed that the frequencies considered are sufficiently low that there is less than one half of a fluid wavelength across the pipe diameter. For clarity, the results for the $s = 1$, fluid-dominated, wave are reproduced below. An $e^{i\omega t}$ time dependence is assumed throughout.

2.1. The fluid-borne $s = 1$ wave

For an in-vacuo pipe at low frequencies, the $s = 1$ wavenumber, k_1, is equal to the free field wavenumber, k_f, modified by a term containing the ratio of the fluid impedance to the radial pipe wall impedance.

$$k_1^2 = k_f^2\left(1 + \frac{z_{\text{fluid}}}{z_{\text{pipe}}}\right), \tag{1}$$

where the fluid and pipe stiffness impedance terms are given by $z_{\text{fluid}} = -2iB_f/a\omega$, $z_{\text{pipe}} = \mathrm{i}(\rho h\omega - Eh/a^2\omega)$; B_f is the bulk modulus of the contained fluid; a and h are the radius and thickness of the shell wall respectively ($h \ll a$); ρ and E are the density and Young's modulus of the shell material respectively; and ω is the angular frequency.

At low frequencies, whether or not the pipes are buried, the $s = 1$ wavenumbers may be approximated by Eq. (1). The equation shows that, for a rigid-walled pipe, the $s = 1$ wavenumber is equal to the free field wavenumber. As the flexibility of the pipe wall increases, the $s = 1$ wavenumber increases, and the wavespeed of the $s = 1$ wave decreases correspondingly. The effect of a lossy pipe wall material (represented by a complex

Young's modulus) is to introduce a negative imaginary component into the wavenumber, indicating that the $s = 1$ wave decays as it propagates.

For sufficiently soft-walled pipes, Eq. (1) may be further approximated by

$$k_1^2 = k_f^2\left(\frac{2B_f a}{Eh}\right). \tag{2}$$

3. Wave behaviour at a flexible side branch

3.1. Wave transmission and reflection

In this section, the wave behaviour at a flexible side branch, as shown in Fig. 1, is examined. The diameter of the sidebranch is assumed to be small compared with the diameter of the main pipe. Both pipes are considered to be of semi-infinite extent downstream of the junction. An axisymmetric ($n = 0$) fluid-dominated ($s = 1$) wave is incident at the pipe junction, and is denoted by P_i. The fluid pressure incident at the junction will be both partially transmitted down the main pipe, P_t, into the sidebranch, P_b, and reflected in the main pipe, P_r, as an $n = 0$, $s = 1$ wave. In addition, there may be some mode conversion at the junction, leading to other modes (e.g. the $n = 0$, $s = 2$ (shell dominated) wave and $n = 1$ bending waves). However, previous work on axisymmetric pipe discontinuities by Muggleton and Brennan [11] has demonstrated that unless there is significant axial loading on the fluid by the shell (or vice versa), such as at a large change in pipe/fluid cross-section, there is no mechanism available to allow mode conversion to occur, so the different modes may be considered independently. In the case considered here, as the diameter of the sidebranch is small compared with the main pipe, the change in total fluid cross-section at the junction is small. Furthermore, motion in the shell wall of the main pipe (both axially and radially) is unlikely to be significantly disrupted by the presence of the sidebranch. The sidebranch will only interrupt a small section of the circumference of the main pipe (also small compared with a wavelength, as frequencies well below the ring frequency are being considered), and, as the sidebranch is flexible, it will not load the main pipe shell to any degree. Some bending waves may be set up in the sidebranch, but as the wall is flexible, the energy associated with these is unlikely to be large compared with the axisymmetric fluid-dominated wave; furthermore, the non-axisymmetric wall motions associated with bending waves will not be picked up by the ring sensor, which only measures axisymmetric motion. Accordingly, a good approximation to the behaviour at the junction can be determined by considering only the $n = 0$, $s = 1$ wave, provided that the correct wavenumbers for each section of pipe are calculated for the coupled problem, as discussed in the previous section. At the junction, therefore, continuity of fluid pressure and fluid volume velocity will apply.

Continuity of fluid pressure gives

$$P_i + P_r = P_t = P_b, \tag{3}$$

where P_i, P_r, P_t and P_b are the acoustic pressures for the incident, reflected, main pipe transmitted and sidebranch transmitted waves respectively.

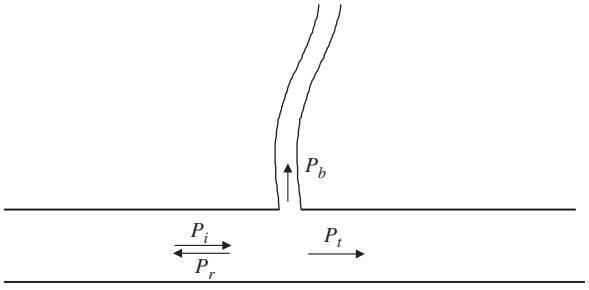

Fig. 1. Diagram showing main pipe/sidebranch configuration and waves P_i, P_r, P_t and P_b denote the complex amplitudes of the incident, reflected, main pipe transmitted and sidebranch transmitted waves, respectively.

Continuity of fluid volume velocity gives

$$(U_i + U_r)a_p^2 = U_t a_p^2 + U_b a_b^2, \tag{4}$$

where a_p and a_b are the radii of the main and branch pipes respectively, and U_i, U_r, U_t and U_b are the particle velocities for the four waves described above.

The particle velocities are related to the pressures via the respective $s = 1$ wavenumbers k_{1p} and k_{1b} in the main pipe and side branch respectively, so that

$$U_i = \frac{k_{1p}}{\rho_f \omega} P_i, \quad U_r = -\frac{k_{1p}}{\rho_f \omega} P_r, \quad U_t = \frac{k_{1p}}{\rho_f \omega} P_t, \quad U_b = \frac{k_{1b}}{\rho_f \omega} P_b. \tag{5a–d}$$

Solving Eqs. (3)–(5) for the reflected and transmitted pressures gives

$$P_r = \frac{-1}{2(k_{1p}a_p^2/k_{1b}a_b^2) + 1} P_i, \quad P_t = P_b = \frac{1}{1 + 1/2(k_{1b}a_b^2/k_{1p}a_p^2)} P_i. \tag{6a,b}$$

Using Eq. (2) the ratio $k_{1b}a_b^2/k_{1p}a_p^2$ in Eq. (6) can be written as

$$\frac{k_{1b}a_b^2}{k_{1p}a_p^2} \approx \left(\frac{a_b^5 h_p E_p}{a_p^5 h_b E_b}\right)^{1/2}, \tag{7}$$

where the subscripts p and b refer to the main pipe and the sidebranch, respectively. This ratio, shown in Table 1 for some typical pipe parameters, will be small compared with unity provided that $h_b E_b / h_p E_p \gg a_b^5/a_p^5$, which is likely for most practical cases. Under these conditions, Eqs. (6a,b) become

$$P_r \approx -\frac{1}{2}\frac{k_{1b}a_b^2}{k_{1p}a_p^2} P_i, \quad P_t = P_b \approx P_i, \tag{8a,b}$$

i.e., very little reflection occurs and almost the full pipe acoustic pressure is transmitted downstream of the junction and into the sidebranch.

3.2. Ring sensor sensitivities

Previous work by Pinnington and Briscoe [4] and Muggleton et al. [5] has shown that the pressure sensitivity, S, of a PVDF ring sensor wrapped around the circumference of a fluid-filled pipe N complete turns is given by

$$S = \frac{2\pi N a a_{\max}}{Eh} S_{\text{ext}}, \tag{9}$$

Table 1
Ring sensor sensitivity and wavenumber ratios for various pipe parameters

Radius ratio	Wall thickness ratio	Young's modulus ratio	$k_{1b}a_b^2/k_{1p}a_p^2$ (Eq. (7))	Sensitivity ratio (equal no. of turns)	Sensitivity ratio (equal wire length)	Wavenumber ratio k_{1b}/k_{1p}
$\frac{a_b}{a_p}$	$\frac{h_b}{h_p}$	$\frac{E_b}{E_p}$	$\left(\frac{a_b^5 h_p E_p}{a_p^5 h_b E_b}\right)^{\frac{1}{2}}$	$\frac{S_b}{S_p} = \frac{a_b^2 E_p h_p}{a_p^2 E_b h_b}$	$\frac{S_b}{S_p} = \frac{a_b E_p h_p}{a_p E_b h_b}$	$\left(\frac{a_b E_p h_p}{a_p E_b h_b}\right)^{\frac{1}{2}}$
0.1	0.1	1 (same pipe material)	0.01	0.1	1	1
0.1	0.1	0.1	0.03	1	10	3
0.1	0.1	0.01 (e.g. hard rubber/MDPE)	0.1	10	100	10
0.1	0.1	10^{-3} (e.g. soft rubber/MDPE)	0.3	100	1000	30
0.13	0.27	0.1 (polythene/MDPE)	0.04	0.6	4.8	2.3

where S_{ext} is the extension sensitivity of the PVDF wire, a is the mean pipe radius, a_{max} is the maximum pipe radius, and E and h are as defined previously. For thin-walled shells, $a_{max} \approx a$, giving

$$S = \frac{2\pi N a^2}{Eh} S_{ext}. \tag{10}$$

Consider a sensor located on the sidebranch and one on the main pipe just downstream of the pipe junction. If the two sensors have the same number of turns, the ratio of the sensitivity of the sidebranch sensor, S_b, compared with that on the main pipe, S_p, is given by

$$\frac{S_b}{S_p} = \frac{a_b^2 E_p h_p}{a_p^2 E_b h_b}. \tag{11}$$

For the same length of PVDF wire in each sensor, this ratio increases to

$$\frac{S_b}{S_p} = \frac{a_b E_p h_p}{a_p E_b h_b}. \tag{12}$$

These two sensitivity ratios are shown in Table 1 for various pipe parameters (the last row shows these ratios for the pipes used in the experiments described in the following section). The table shows that, provided the sidebranch wall material is sufficiently soft compared with the main pipe wall material, substantial sensitivity gains can be made by using a sensor placed on the sidebranch; even if the same wall material is used for the sidebranch, there is no loss in pressure sensitivity as long as the same overall length of wire is used.

Unfortunately, the sensitivities shown in the table can never be fully realized. Eq. (10), giving the sensor sensitivity in terms of the pipe parameters, neglects the stiffness of the sensor itself, which will become increasingly important for softer pipes. If the stiffness of the sensor is included, it can been shown (see Appendix A) that the sensitivity is modified by a term which can be interpreted as the ratio of the radial stiffness of the wire to the radial stiffness of the pipe wall.

$$S_{mod} = \frac{S}{1 + \frac{E_w h_w}{Eh}\left(\frac{a}{a + \frac{h+h_w}{2}}\right)^2}, \tag{13}$$

where S_{mod} is the modified pressure sensitivity and E_w and h_w are the Young's modulus and thickness of the wire, respectively. For very soft-walled pipes, the additional term may be large, indicating that the wire stiffness dominates. In the limit the pressure sensitivity becomes that of the wire alone.

$$S_w = \frac{2\pi N\left(a + \frac{h+h_w}{2}\right)^2}{E_w h_w} S_{ext}. \tag{14}$$

This represents the upper limit for the sensitivity that can be achieved with any given wire on a pipe with given dimensions.

Increased sensitivity can, of course, be achieved by increasing the number of wire turns, with the limit being set by the need for the overall spread of the sensor along the pipe length to be small compared with a wavelength. The gain that can be achieved for pipes of given dimensions will also be bounded by the fact that as the pipe wall stiffness ratio, E_p/E_b, increases, Eq. (8) will no longer be valid; more energy will be reflected back down the main pipe, and the pressure transmitted to the sidebranch and downstream in the main pipe will start to fall. Fig. 2 shows the reflected and transmitted pressures as a function of the ratio $k_{1b}a_b^2/k_{1p}a_p^2$ given by Eq. (6), along with the approximations given in Eq. (8), where these trends can be seen. For values of the ratio $k_{1b}a_b^2/k_{1p}a_p^2$ up to around 0.1, Eq. (8) gives good approximations to the reflection and transmission coefficients; for values up to around unity, the reflection and transmission coefficients are of the same order as the approximations; for values above unity, Eq. (8) is no longer valid.

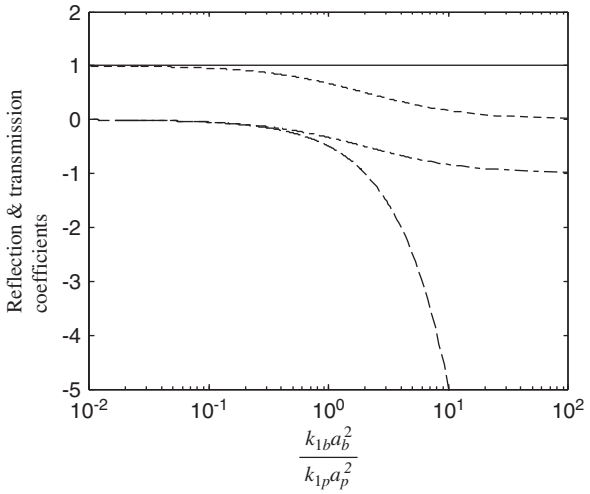

Fig. 2. Reflection and transmission coefficients at the sidebranch and their approximations (Eqs. (6a,b) and (8a,b)). - - - - - - - reflection coefficient; – – – – approximation, …… transmission coefficient; —— approximation.

4. Experimental measurements

4.1. Experimental set-up and procedure

Measurements to support the theoretical findings have been made on a water-filled pipe in the laboratory. The experimental arrangement is shown in Figs. 3a and b. It consisted of a water-filled medium density polyethylene (MDPE) pipe, approximately 2 m in length, secured vertically, with the lower end sealed. A polythene sidebranch, again approximately 1.5 m in length, was fitted to the main pipe approximately half way along its length, as can be seen from Fig. 3a. The external diameters of the main pipe and sidebranch were 180 and 25 mm respectively, with the wall thicknesses being 11 and 3.0 mm, respectively. The main pipe was instrumented with five calibrated two-turn pressure-sensing PVDF wire ring transducers, as described in Ref. [5] three upstream of the sidebranch (equispaced), and two downstream of it; the sidebranch was instrumented with three fourteen-turn equispaced transducers (approximately the same wire length as the sensors on the main pipe). The five transducers in the main pipe and the three in the sidebranch allowed for decomposition of outgoing and returning waves in each section of the piping system as well as enabling the respective wavenumbers to be determined [6,8]. Decomposition of the waves was necessary as both the main pipe and the sidebranch were finite and neither was anechoically terminated. In addition a B&K 8103 hydrophone was inserted into the sidebranch in line with one of the PVDF wire rings, in order to calibrate the ring sensors in the sidebranch (those in the main pipe had been calibrated previously); a hydrophone was also placed in the main pipe at the level of the sidebranch.

The water column was excited at the upper end by an electrodynamic shaker attached to a light, rigid piston (Fig. 3b). The piston was excited with a swept sine input from 30 to 500 Hz, and the signals from the transducers subsequently analyzed.

4.2. Experimental results and comparison with theory

4.2.1. Measured wavenumbers

The measured wavenumbers in the main pipe and in the sidebranch were calculated using the three transducer method described previously by [6], as this method allows for unknown boundary conditions at either end of the pipe. Good comparisons between measured data and theoretical predictions based on measured values of the pipe elastic properties for the main pipe have been demonstrated and reported previously [6] and are not shown here. Material data is not readily available for the sidebranch polythene, and, being considerably softer than MDPE, difficult to measure by the direct method used for the MDPE [5].

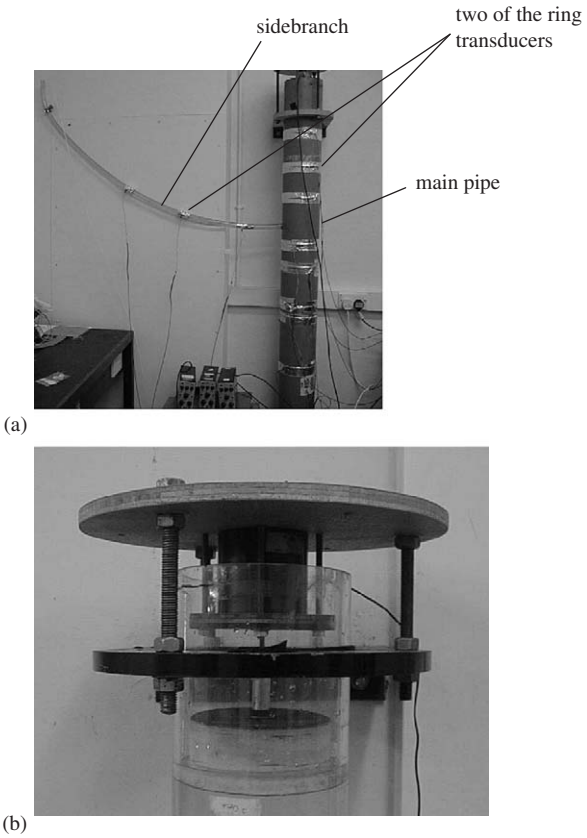

Fig. 3. Experimental setup (a) instrumented MDPE pipe; (b) close-up of exciter (shown here on a perspex pipe for clarity).

However, from the measured wavenumbers in the sidebranch, the Young's modulus and loss factor can be inferred.

The real and the imaginary components of the measured wavenumbers are shown in Figs. 4a and b. The imaginary part is expressed as wave attenuation in dB/m where

$$\text{Loss (dB/m)} = \frac{20\,\text{Im}\{k\}}{\ln(10)}.$$

Least squares straight-line fits passing through the origin are also shown on both plots, indicating, from Fig. 4a, a wavespeed of approximately 150 m/s. These straight-line fits can be used to estimate the elastic properties of the polythene. Substituting the fits and the pipe dimensions into Eq. (2), the Young's modulus is found to be approximately $1.6 \times 10^8\,\text{N/m}^2$, with the loss factor being approximately 0.65.

4.2.2. Side branch sensor sensitivity

Table 2 shows the material properties and dimensions of the PVDF wire and the polythene sidebranch. Using Eq. (9), the pressure sensitivity of a 14-turn transducer on the sidebranch is found to be 5.42 pC/Pa. This reduces to 1.05 pC/Pa once the stiffness of the wire is included (Eq. (14)) showing clearly that the wire stiffness dominates.

Figs. 5a and b show the magnitude and unwrapped phase of the pressure measured by the PVDF wire on the sidebranch and the collocated hydrophone. Both are normalized by the pressure measured at the nearest transducer to the exciter (p_0); the peaks and troughs in the response arise as a result of this normalization rather than inadequate wave decomposition (see discussion in Section 4.2.4 showing that there is almost no returning wave in the sidebranch). The figures show that, whilst the two sensors show the same pressure

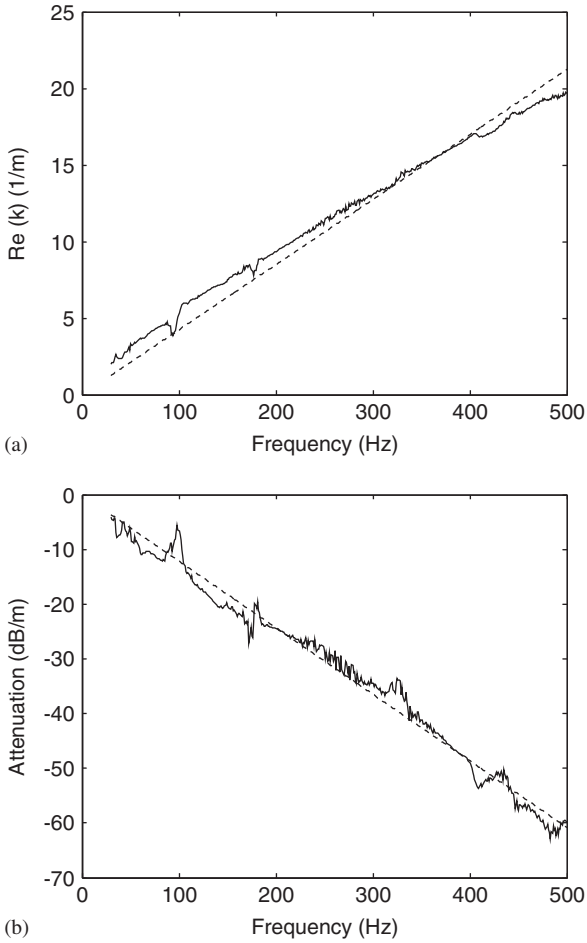

Fig. 4. Measured wavenumber in sidebranch (a) real part, (b) imaginary part. ———measured data; - - - - - - - - - least squares fit.

Table 2
Properties of PVDF wire and sidebranch

	Young's modulus E (N/m^2)	Mean radius a (mm)	Maximum radius a_{max} (mm)	Thickness h (mm)	$2B_f a/Eh$
Polythene sidebranch	1.6×10^8	11.0	12.5	3.0	103
PVDF wire (strain sensitivity 2.15×10^8 pC/m)	2.0×10^9	—	—	1.45	

magnitude trends, and there is good agreement in the measured phase, the absolute pressure values are not in agreement. The PVDF wire sensor is not as sensitive as predicted (even allowing for the stiffness of the wire), a factor of approximately 2.5 being required in order for the wire and hydrophone measurements to agree (see Fig. 6), and for the same length of wire only about half as sensitive as a sensor located on the main pipe. However, this sensitivity is still approximately four times greater than the hydrophone used for comparison (B&K type 8103).

There are several possible reasons for the wire being not as sensitive as predicted. It is already known that the approximations implied by Eqs. (2, 7 and 8) are valid (see Tables 1 and 2) so clearly these are not the cause of the discrepancy. In calculating the wire sensitivity it was assumed that the strain experienced by the pipe

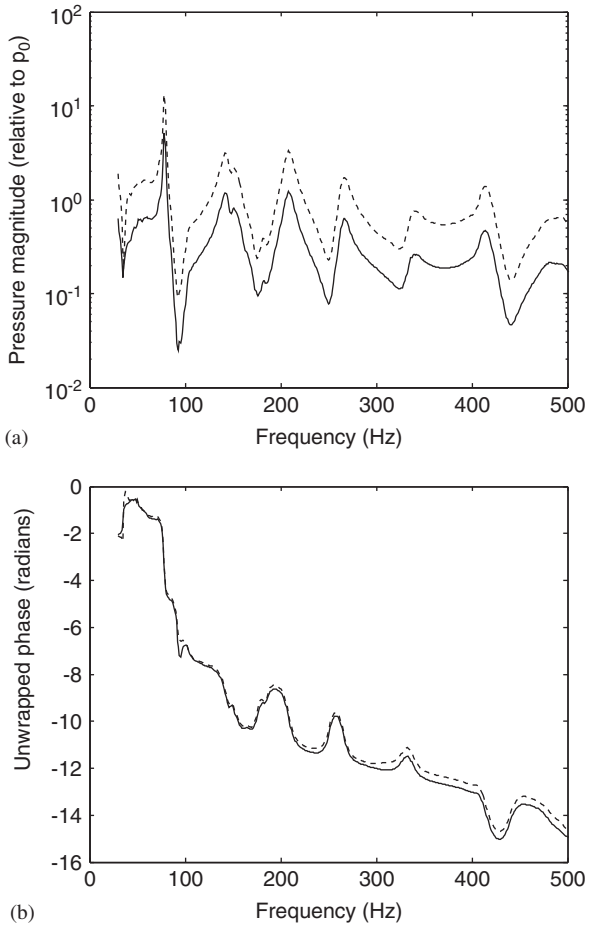

Fig. 5. Measured pressure in sidebranch (a) magnitude, (b) unwrapped phase. ——— PVDF wire data using predicted sensitivity; - - - - - - - - - hydrophone data.

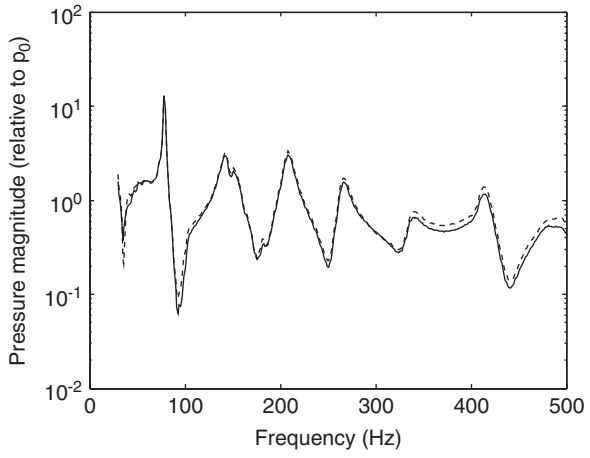

Fig. 6. Magnitude of measured pressure in sidebranch. ——— PVDF wire data using modified sensitivity; - - - - - - - - - hydrophone data.

wall is wholly transmitted to the wire, i.e. that no slippage occurs in the pipe/wire interface, and that no pipe bulging occurs, either between the wire turns or either side of the transducer. Significant slippage is unlikely, as the transducers were secured to the pipe with double-sided sticky tape (a proven method used previously [4–6]). Both forms of pipe bulging, however, are likely as the pipe wall radial stiffness for the extremely soft polythene is less than that of the wire. Neither of these effects is easily quantifiable, and further analysis is beyond the scope of this paper. In the following sub-sections, the measured wire sensitivity including the factor of 2.5 has been used in the analyses.

4.2.3. Waves in the main pipe

Eq. (8) predicts that, at the level of the sidebranch, very little reflection occurs in the main pipe, and that almost all the acoustic pressure is transmitted further along the main pipe, i.e. the sidebranch is almost invisible to the main pipe. The intention here, therefore, is to show that the acoustic pressure magnitudes of the outgoing and returning waves downstream of the sidebranch in the main pipe were similar to those upstream. Figs. 7a and b show the magnitude and unwrapped phase of the outgoing waves in the main pipe upstream and downstream of the sidebranch (normalized by the pressure at the sensor nearest the exciter—again the cause of the peaky response). The graphs clearly show that, at the frequencies considered, the sidebranch has negligible effect on the pressure transmitted downstream in the main pipe, thus confirming the theoretical predictions. Comparison of the returning waves just before and just after the junction revealed similar behaviour.

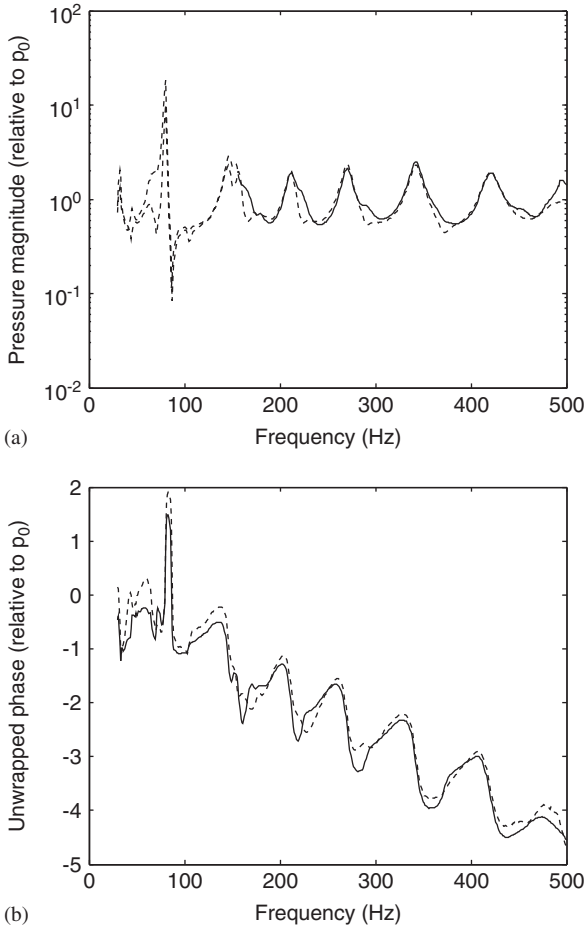

Fig. 7. Outgoing waves in main pipe upstream and downstream of sidebranch (a) Magnitude; (b) unwrapped phase. ——— Upstream of sidebranch; - - - - - - - - - downstream of sidebranch.

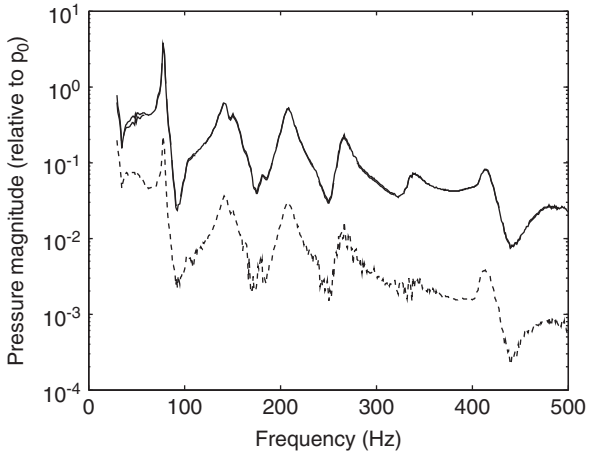

Fig. 8. Magnitude of waves in sidebranch (at position of middle sensor) ——— outgoing wave; - - - - - - - - - returning wave; – – – – – middle sensor (barely distinguishable from outgoing wave trace).

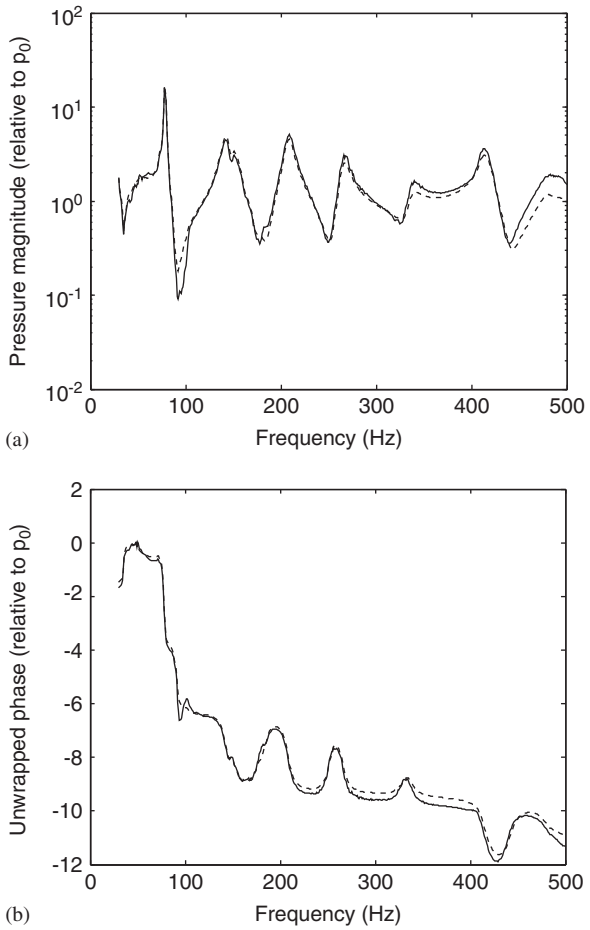

Fig. 9. Acoustic pressure in main pipe and transmitted into sidebranch (a) Magnitude; (b) unwrapped phase. ——— sidebranch using wire data; - - - - - - - - - main pipe using hydrophone data.

4.2.4. Waves in the sidebranch

Eq. (8) also predicts that the acoustic pressure is transmitted effectively into the sidebranch from the main pipe. Fig. 8 shows the magnitudes of the outgoing and returning waves in the sidebranch, as measured by the PVDF wire, calculated at the position of the middle sensor. Also shown is the pressure measured at the middle sensor. The graph shows that the wave attenuation over the sidebranch length is sufficiently large for the magnitude of the returning wave to be negligible compared with that of the outgoing wave, i.e. the sidebranch can be considered to be anechoically terminated, and the measured pressures consist of outgoing waves only. Figs. 9a and b show the magnitudes and unwrapped phase of the pressure measured in the sidebranch, back-propagated to the main pipe/sidebranch junction using the measured wavenumber in the sidebranch. The pressure measured by the hydrophone in the main pipe at this junction is also shown. The figures show good agreement, both for the magnitude and the phase of the measured pressures. This demonstrates that, as predicted, the acoustic pressure transmits effectively from the main pipe into the sidebranch.

5. Summary

In this paper, a low-frequency theoretical model of a flexible sidebranch connected to a fluid-filled pipe has been formulated, with a view to developing a sensitive pressure sensor using PVDF wire wrapped around the sidebranch. The model predicts that the acoustic pressure in the main pipe transmits well into the sidebranch, whilst the pressure in the main pipe is largely unaffected. This suggests that PVDF wire located on the sidebranch will effectively monitor the pressure in the main pipe. Moreover, if the sidebranch stiffness is matched to that of the wire, substantial sensitivity gains can be made using this configuration compared with locating the wire on the main pipe.

Measurements have been made in the laboratory on a MDPE finite pipe with a polythene sidebranch connected to it. The measurements confirm that the acoustic pressure is transmitted effectively into the sidebranch as well as further down the main pipe. The wave attenuation in the side branch was found to be large enough for the acoustic pressure in the main pipe to be monitored using a single sensor on the sidebranch, once the wavespeed and attenuation in the sidebranch had been determined.

The pressure sensitivity of a PVDF wire sensor on the sidebranch was measured and compared with the theoretically predicted value. It was found that the stiffness of the wire limited the sensitivity, which could be achieved, and that the measured sensitivity was substantially less than predicted, even accounting for the wire stiffness. This was thought to be primarily as a result of pipe bulging either side of the sensor and between the sensor turns, the bulging being likely to occur when the radial pipe wall stiffness is less than the wire stiffness.

The proposed sensor is a promising alternative to a conventional hydrophone for measuring the acoustic pressure in a buried water pipe, although some considerable development work is required before it could be used in the field. Further work would be needed to determine the effect of the connection between the main pipe and the sensor pipe (for example a fire hydrant) in a real network (particularly the effect of additional discontinuities at the junction not modelled here), and to examine the other issues associated with connecting to a live main (e.g. static pressure and flow). Alternative PVDF wires could also be investigated to determine the maximum sensitivity that can be achieved in practice, along with the more practical issues of sensor deployment, reliability, ease of use and, of course, cost.

Acknowledgement

The EPSRC are gratefully acknowledged for their support of this work.

Appendix A. Ring sensor sensitivity for a soft-walled pipe

Data on the PVDF wire supplied by the manufacturer, Ormal Ltd, is in the form of piezoelectric charge coefficient, e31, and the diameters of the core and whole wire, X and Y respectively, as shown in Table A1 for the wire used in this study.

The piezoelectric charge coefficient is related to the charge generated by the wire, Q, the longitudinal strain, $\Delta L/L$, and the effective electrode area, A, by [12]

$$e_{31} = \frac{Q}{\Delta L/L}\frac{1}{A}, \tag{A.1}$$

where

$$A = \frac{\pi L(Y-X)}{\ln(Y/X)}. \tag{A.2}$$

The charge per unit extension of the wire, $Q/\Delta L$, is therefore given by

$$\frac{Q}{\Delta L} = e_{31}\pi\frac{(Y-X)}{\ln(Y/X)}. \tag{A.3}$$

For the axisymmetric 'fluid-borne' wave in a fluid-filled pipe, at low frequencies, where there is less than one half of a fluid wavelength across the pipe diameter, the magnitude of the radial extension of the pipe wall, W, is related to the magnitude of the internal pressure in the fluid, P, via [7]

$$P = -\frac{2\omega^2\rho_f}{(k_f^r)^2 a}W, \tag{A.4}$$

where ρ_f is the fluid density, a is the mean pipe radius, and k_f^r is the radial fluid wavenumber, related to the fluid wavenumber, k_f, and axial wavenumber, k, by

$$(k_f^r)^2 = k_f^2 - k^2. \tag{A.5}$$

Muggleton et al. [7] also showed that, at low frequencies, in the absence of a surrounding medium, the axial wavenumber, k, is related to the fluid wavenumber, k_f, by

$$k^2 = k_f^2\left(1 + \frac{2B_f a}{Eh}\right), \tag{A.6}$$

where B_f is the bulk modulus of the contained fluid, E is the elastic modulus of the pipe wall, and h is the pipe wall thickness.

Substituting Eqs. (A.5) and (A.6) into Eq. (A.4), and rearranging gives

$$P = \frac{Eh}{a^2}W. \tag{A.7}$$

This is the static relationship between internal pressure and radial displacement for a ring, where Eh/a^2 is the radial stiffness of the pipe wall.

If a wire is wrapped N times around the pipe circumference, the extension of the wire, w_{ext}, is related to the mean radial displacement of the pipe wall, W, by

$$w_{\text{ext}} = 2\pi N\frac{a_{\max}}{a}W, \tag{A.8}$$

where $a_{\max}$ is the outer pipe wall radius.

Furthermore, if S_{ext} is the charge sensitivity of the wire per unit extension, the pressure sensitivity of the wire S (charge per unit pressure within the pipe) is, from Eqs. (A.7) and (A.8), given by

$$S = \frac{2\pi N a a_{\max}}{Eh}S_{\text{ext}}. \tag{A.9}$$

Table A1
PVDF wire constants as supplied by Ormal Ltd

Wire type	e_{31} (pC/m^2)	Y (m)	X (m)	Charge/extn (pC/m)
Vibetek 20	8.0×10^{10}	1.45×10^{-3}	0.45×10^{-3}	2.15×10^{8}

However, Eqs. (A.7) and (A.9) neglect the stiffness of the wire, which maybe significant for soft-walled pipes. Including the wire stiffness, Eq. (A.7) becomes

$$P = \left(\frac{Eh}{a^2} + \frac{E_w h_w}{a_w^2}\right) W, \tag{A.10}$$

where E_w, h_w, and a_w are the Young's modulus, thickness and radius respectively of the wire ring.

Substituting Eq. (A.10) into Eq. (A.8), and rearranging, assuming that the wire thickness is small compared with the pipe radius, gives the modified pressure sensitivity as

$$S_{\text{mod}} = \frac{S}{1 + \frac{E_W h_W}{Eh}\left(\frac{a}{a + \frac{h+h_w}{2}}\right)^2}. \tag{A.11}$$

References

[1] H.V. Fuchs, R. Riehle, Ten years of experience with leak detection by acoustic signal analysis, *Applied Acoustics* 33 (1991) 1–19.
[2] O. Hunaidi, W.T. Chu, Acoustical characteristics of leak signals in water distribution pipes, *Applied Acoustics* 58 (1999) 235–254.
[3] O. Hunaidi, W.T. Chu, A. Wang, W. Guan, Detecting leaks in plastic water distribution pipes, *Journal of the American Water Works Association* 92 (2000) 82–94.
[4] R.J. Pinnington, A.R. Briscoe, Externally applied sensor for axisymmetric waves in a fluid filled pipe, *Journal of Sound and Vibration* 173 (1994) 503–516.
[5] J.M. Muggleton, M.J. Brennan, R.J. Pinnington, Development of a water pipe monitoring system for leak detection: experimental work, *ISVR Technical Memorandum* 860 (2001).
[6] J.M. Muggleton, M.J. Brennan, P.W. Linford, Axisymmetric wave propagation in fluid-filled pipes: wavenumber measurements in in-vacuo and buried pipes, *Journal of Sound and Vibration* 270 (2004) 171–190.
[7] J.M. Muggleton, M.J. Brennan, R.J. Pinnington, Wavenumber prediction of waves in buried pipes for water leak detection, *Journal of Sound and Vibration* 249 (2002) 939–954.
[8] J.M. Muggleton, M.J. Brennan, Leak noise propagation and attenuation in submerged plastic water pipes, *Journal of Sound and Vibration* 278 (2004) 527–537.
[9] C.R. Fuller, F.J. Fahy, Characteristics of wave propagation and energy distributions in cylindrical elastic shells filled with fluid, *Journal of Sound and Vibration* 81 (1982) 501–518.
[10] E.H. Kennard, The new approach to shell theory: circular cylinders, *Journal of Applied Mechanics* (1953) 33–40.
[11] J.M. Muggleton, M.J. Brennan, Axisymmetric wave propagation in buried, fluid-filled pipes: effects of wall discontinuities, *Journal of Sound and Vibration* 281 (2005) 849–867.
[12] M. Redman, Private communication, Ormal Ltd., 2001.